Electronic Supplementary Material (ESI) for New Journal of Chemistry.

Modulating Intrinsic Properties of Platinum-Cobalt Nanowires for Enhanced Electrocatalysis of oxygen reduction reaction

Fangfang Chang[a], Yongpeng Liu[a], Lin Yang[a], Qing Zhang[a], Juncai Wei[a], Xiaolei Wang[b] and Zhengyu Bai [a]*

[a]Collaborative Innovation Center of Henan Province for Green Manufacturing of Fine Chemicals, Key Laboratory of Green Chemical Media and Reactions, Ministry of Education, School of Chemistry and Chemical Engineering, Henan Normal University, Xinxiang, Henan 453007, China. Email: baizhengyu2000@163.com;

[b]Department of Chemical and Materials Engineering, University of Alberta, Edmonton, Alberta T6G 1H9, Canada.

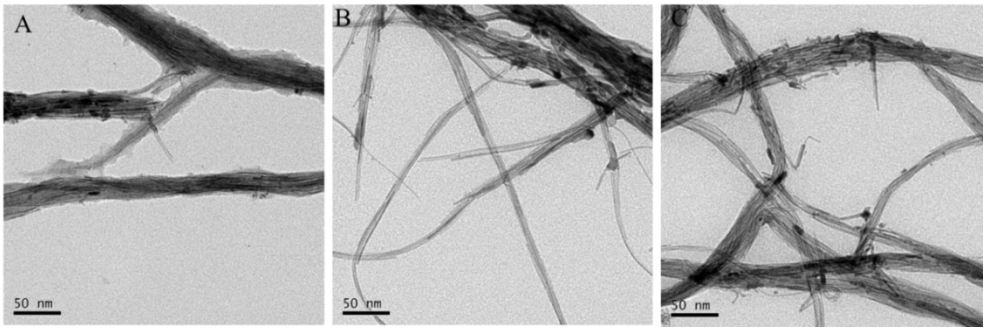

Fig. S1. TEM images of the nanowire samples $Pt_{23}Co_{77}$(A), $Pt_{57}Co_{43}$ (B) and $Pt_{70}Co_{30}$(C).

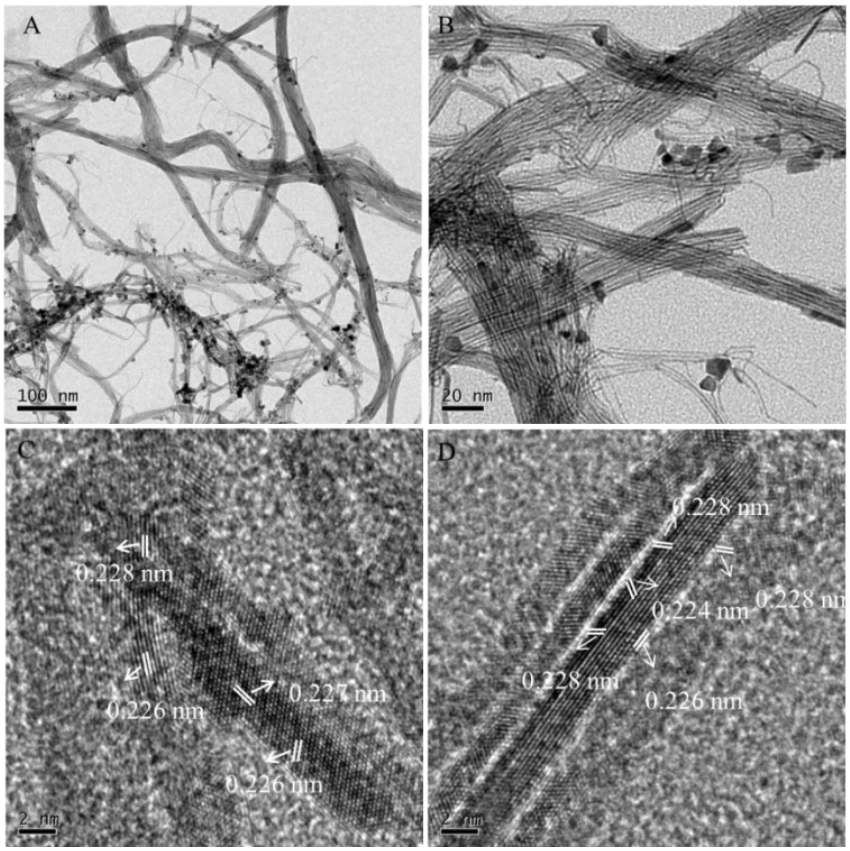

Fig. S2. TEM images (A-B) and HR-TEM images (C-D) of Pt NWs

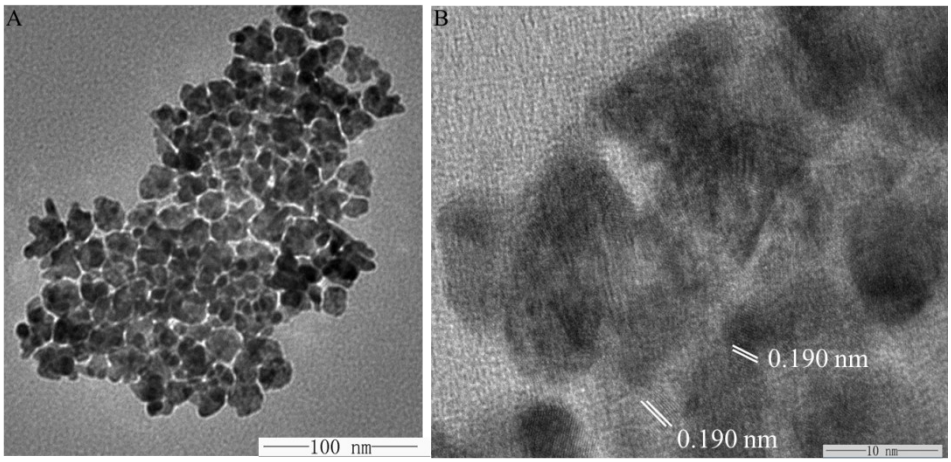

Fig. S3. TEM images of $Pt_{70}Co_{30}$ NPs

Table S1. Summary of NWs Sizes and Lattice Constants for Pt_nCo_{100-n}/C alloy catalysts

Catalysts	NWs size (nm)	Metal loading (% wt)	Lattice parameter(nm)	Scherrer size (nm)
$Pt_{23}Co_{77}$/C	2.4±0.5	15.0%	0.3650	2.6±0.3
$Pt_{57}Co_{43}$/C	2.1±0.3	12.0%	0.3740	2.3±0.5
$Pt_{70}Co_{30}$/C	1.8±0.4	12.5%	0.3790	2.1±0.4
Pt/C	2.0±0.7	15.0%	0.3920	2.3±0.5

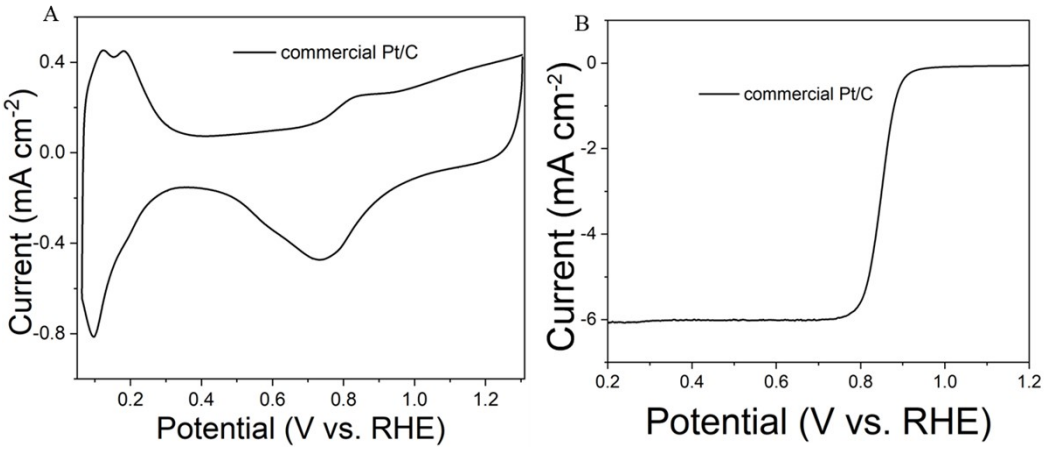

Fig. S4. CV (A) and RDE (B) curves for commercial Pt/C in 0.1 M $HClO_4$ solution saturated with nitrogen (scan rate: 50 mV/s) and oxygen (scan rate: 10 mV/s and rotation speed: 1600 rpm)

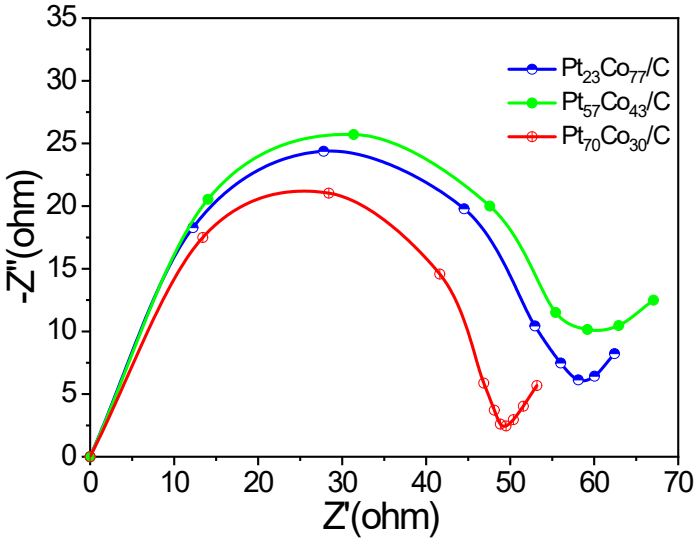

Fig. S5. EIS plots of the $Pt_{23}Co_{77}$/C, $Pt_{57}Co_{43}$/C and $Pt_{70}Co_{30}$/C, respectively.

Table S2. Comparison of compositions, and ORR activities for different PtCo alloy catalysts

Catalyst	Electrolyte	Mass Activity (A/mg_{Pt}[-1])	Specific Activity(mA/cm^2)	Reference
PtCo NRAs	0.1 M $HClO_4$	0.194	1.854	1
Au/Pt-Co/C	0.1 M $HClO_4$	0.62	1.43	2
PtCo MNs	0.1M $HClO_4$	0.72	0.91	3
Pt-Co	0.1 M $HClO_4$	0.53	0.8	4
Pt-Co GB-NWs/C-OCP	0.1M $HClO_4$	1.31	1.55	5
$Pt_{70}Co_{30}$/C	0.1M $HClO_4$	2.3	4.1	This work

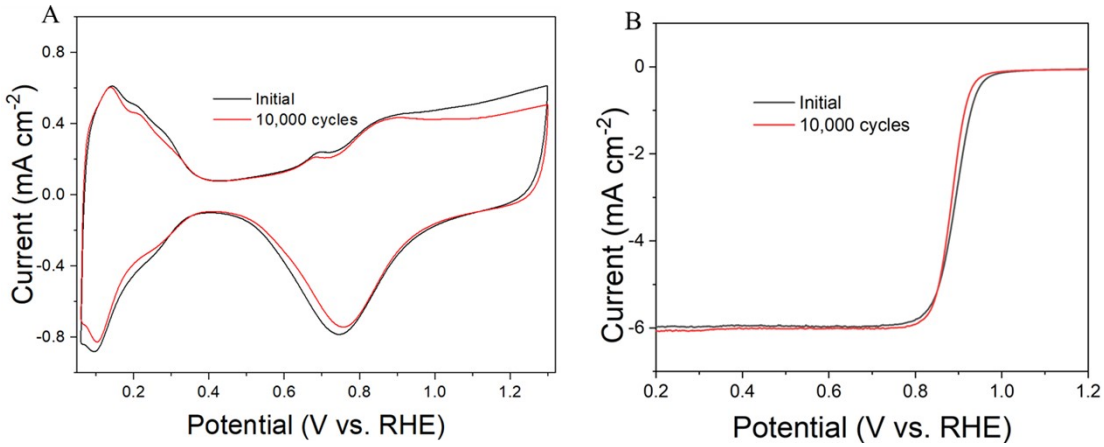

Fig. S6. CV (A) and RDE (B) curves for commercial Pt/C before and after 10,000 potential cycles (sweep rate, 100mV/s, potential cycle window: 0.6 and 1.1 V) in 0.1 M $HClO_4$ solution saturated with nitrogen (scan rate: 50 mV/s) and oxygen (scan rate: 10 mV/s and rotation speed: 1600 rpm).

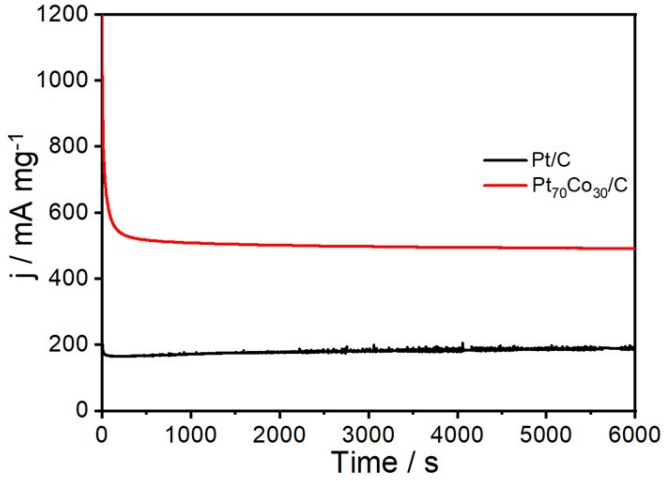

Fig. S7. Chronoamperometric curves (CAs) of the glassy carbon electrodes coated by $Pt_{70}Co_{30}$/C and commercial Pt/C catalysts measured in 0.1 M $HClO_4$ solution saturated with nitrogen

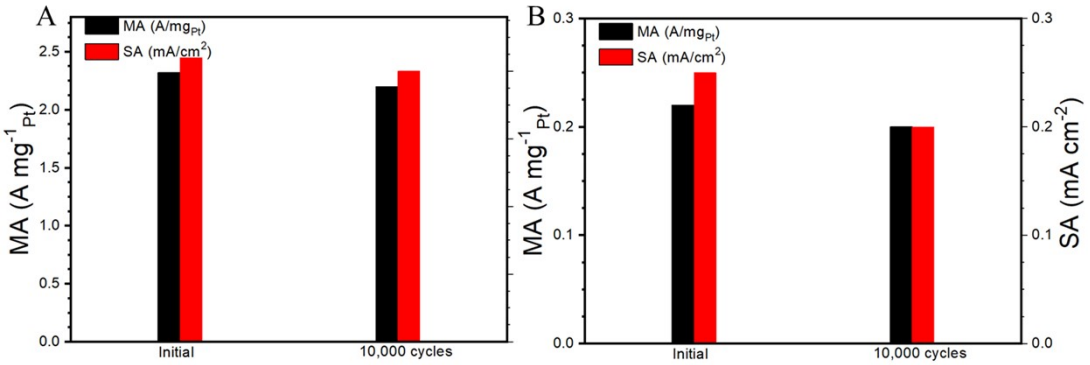

Fig. S8. Mass activity and specific activity data $Pt_{70}Co_{30}$/C NWs (A) and commercial Pt/C (B) at 0.900 V (vs. RHE) before and after 10,000 cycles.

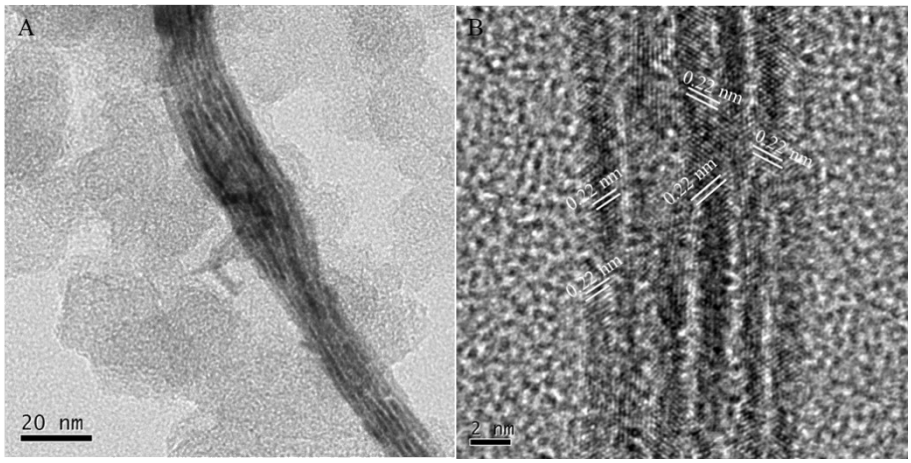

Fig. S9. TEM (A) and HR-TEM (B) images for $Pt_{70}Co_{30}$/C after 10,000 cycles

Table S3. The electron configuration and natural atomic charge of the optimized structure of Pt_nCo_{4-n} (n=1, 2, 3, 4) clusters

cluster	atom No	electron configuration	charge	e-transfer
	1Pt	$6S^{0.57}5d^{9.41}6p^{0.08}$	0.00	
Pt_4	2Pt	$6S^{0.57}5d^{9.41}6p^{0.08}$	0.00	

	3Pt	$6S^{0.68}5d^{9.16}6p^{0.12}$	0.00	
	4Pt	$6S^{0.68}5d^{9.16}6p^{0.12}$	0.00	
	1Co	$4S^{0.20}3d^{2.90}4p^{0.08}$	0.48	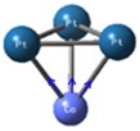
Pt_3Co_1	2Pt	$6S^{0.34}5d^{4.85}6p^{0.05}$	-0.16	
	3Pt	$6S^{0.37}5d^{4.87}6p^{0.05}$	-0.16	
	4Pt	$6S^{0.37}5d^{4.87}6p^{0.05}$	-0.16	
	1Co	$4S^{0.57}3d^{7.90}4p^{0.13}5p^{0.14}$	0.23	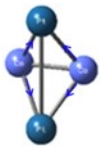
Pt_2Co_2	2Pt	$6S^{1.05}5d^{9.18}6p^{0.03}$	-0.23	
	3Pt	$6S^{1.05}5d^{9.18}6p^{0.03}$	-0.23	
	4Co	$4S^{0.57}3d^{7.90}4p^{0.13}4d^{0.01}5p^{0.14}$	0.23	
	1Co	$4S^{0.26}3d^{3.94}4p^{0.08}$	0.14	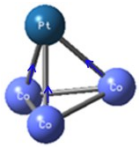
Pt_1Co_3	2Pt	$6S^{0.38}5d^{4.73}6p^{0.04}$	-0.42	
	3Co	$4S^{0.26}3d^{3.94}4p^{0.08}$	0.14	
	4Co	$4S^{0.26}3d^{3.94}4p^{0.08}$	0.14	

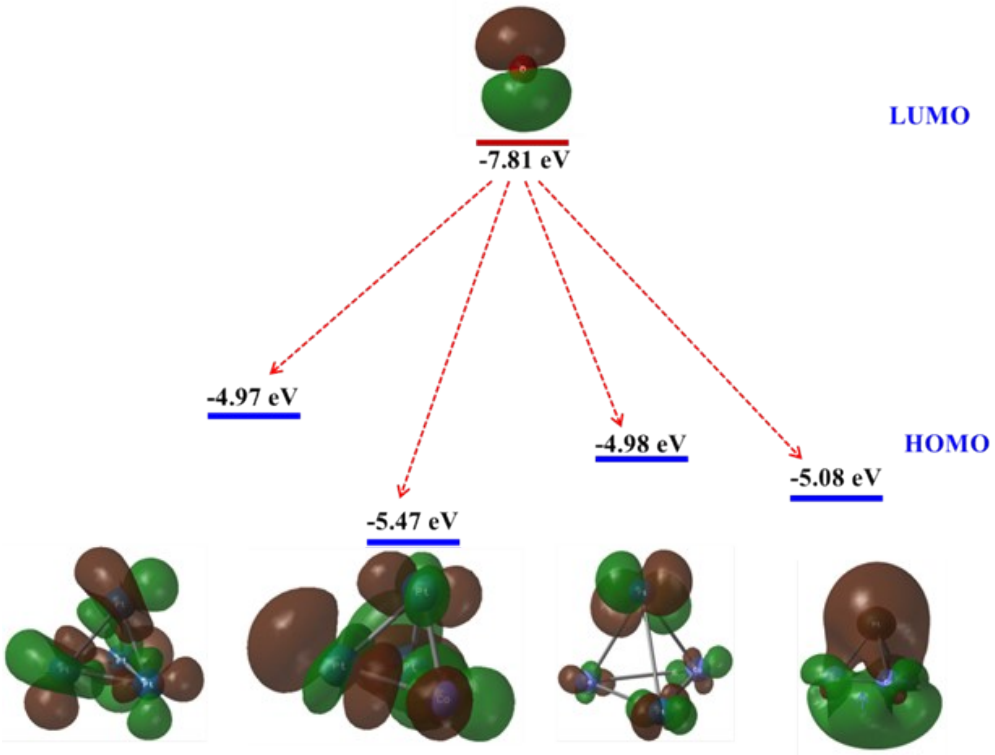

Fig. S10 Frontier molecular orbitals and the energy of LUMO of O atom and HOMO of Pt_nCo_{4-n} (n = 4, 3, 2, 1) clusters

Table S4. Structure and adsorption energy (eV) for O on Pt_nCo_{10-n} (n=2, 6, 7, 10) clusters

	Pt_2Co_8	Pt_6Co_4	Pt_7Co_3	Pt_{10}
	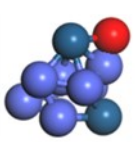	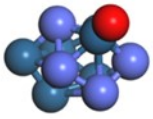	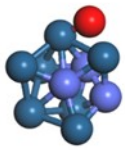	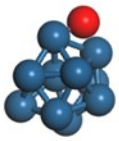
O	-2.30	-2.12	-1.95	-1.91

Table S5. Structure and adsorption energy (eV) for OH on Pt_nCo_{10-n} (n=2, 6, 7, 10) clusters

	Pt_2Co_8	Pt_6Co_4	Pt_7Co_3	Pt_{10}
	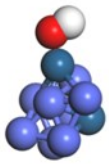		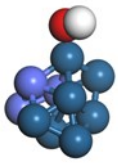	
OH	-1.89	-1.80	-1.78	-1.74

Table S6. Structure and adsorption energy (eV) for OOH on Pt_nCo_{10-n} (n=2, 6, 7, 10) clusters

	Pt_2Co_8	Pt_6Co_4	Pt_7Co_3	Pt_{10}
	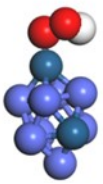	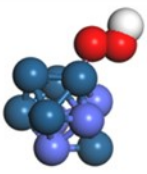	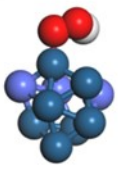	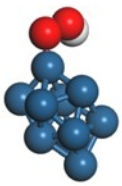
OOH	-1.72	-1.69	-1.65	-1.59

Table S7. The correction of zero point energy and entropy of the adsorbed and gaseous species.

	ZPE(eV)	TS(eV)
*OOH	0.35	0
*O	0.05	0
*OH	0.31	0.01
H_2O	0.56	0.67
H_2	0.27	0.41

Reference:

1 S. -Q. Hu, Z. Wang, H. L. Chen, S. B. Wang, X. G. Li, X. Y. Zhang, P. G. Shen, G. Pei, Ultrathin PtCo nanorod assemblies with self-optimized surface for oxygen reduction reaction. *J. Electroanal. Chem.,* 2020, **870**, 114194.

2 C. Ding, Z. Mao, J.-S. Liang, X. Qin, Q. Zhang, F. Yang, Q. Li, W.-B. Cai, Aqueous phase approach to Au-modified Pt−Co/C toward efficient and durable cathode catalyst of PEMFCs, *J. Phys. Chem. C*, 2021, **125**, 23821−23829.

3 H. J. Wang, H. J. Yu, Y. H. Li, , S. L. Yin, H. Xue, R. X. N. Li, X. You, L. Wang, Direct synthesis of bimetallic PtCo mesoporous nanospheres as efficient bifunctional electrocatalysts for both oxygen reduction reaction and methanol oxidation reaction, *Nanotechnology,* 2018, **29,** 175403.

4 Y. J. Wu, Y. G. Zhao, J. J. Liu, F. Wang, Adding refractory 5d transition metal W into PtCo system: an advanced ternary alloy for efficient oxygen reduction reaction, *J. Mater. Chem. A,* 2018, **6**, 10700-10709.

5 M. Kabiraz, B. Ruqia, J. Kim, H. Kim, Y. Hong, M. Kim, Y. Kim, C. Kim, W.-J. Lee, W. Lee, G. Hwang, H. Cheol Ri, H. Baik, H.-S. Oh, Y. Lee, L. Gao, H. Huang, S. Paek, Y.-J Jo, C. Choi, S. Han, S. Choi, Understanding the grain boundary behavior of bimetallic platinum−cobalt alloy nanowires toward oxygen electroReduction, *ACS Catal*., 2022, **12**, 3516−3523.